

Research Article

Sedoheptulose-1,7-bisphosphate Accumulation and Metabolic Anomalies in Hepatoma Cells Exposed to Oxidative Stress

Mei-Ling Cheng,^{1,2,3} Jui-Fen Lin,² Cheng-Yu Huang,² Guan-Jie Li,⁴ Lu-Min Shih,² Daniel Tsun-Yee Chiu,⁴ and Hung-Yao Ho ^{3,4}

¹Department of Biomedical Sciences, College of Medicine, Chang Gung University, Taoyuan, Taiwan

²Metabolomics Core Laboratory, Healthy Aging Research Center, Chang Gung University, Taoyuan, Taiwan

³Clinical Metabolomics Core Laboratory, Chang Gung Memorial Hospital at Linkou, Taoyuan, Taiwan

⁴Department of Medical Biotechnology and Laboratory Science, College of Medicine, Chang Gung University, Taoyuan, Taiwan

Correspondence should be addressed to Hung-Yao Ho; hoh01@mail.cgu.edu.tw

Received 18 September 2018; Accepted 15 November 2018; Published 13 January 2019

Academic Editor: Grzegorz Bartosz

Copyright © 2019 Mei-Ling Cheng et al. This is an open access article distributed under the Creative Commons Attribution License, which permits unrestricted use, distribution, and reproduction in any medium, provided the original work is properly cited.

We have previously shown that GSH depletion alters global metabolism of cells. In the present study, we applied a metabolomic approach for studying the early changes in metabolism in hydrogen peroxide- (H_2O_2 -) treated hepatoma cells which were destined to die. Levels of fructose 1,6-bisphosphate and an unusual metabolite, sedoheptulose 1,7-bisphosphate (S-1,7-BP), were elevated in hepatoma Hep G2 cells. Deficiency in G6PD activity significantly reduced S-1,7-BP formation, suggesting that S-1,7-BP is formed in the pentose phosphate pathway as a response to oxidative stress. Additionally, H_2O_2 treatment significantly increased the level of nicotinamide adenine dinucleotide phosphate ($NADP^+$) and reduced the levels of ATP and NAD^+ . Severe depletion of ATP and NAD^+ in H_2O_2 -treated Hep G2 cells was associated with cell death. Inhibition of PARP-mediated NAD^+ depletion partially protected cells from death. Comparison of metabolite profiles of G6PD-deficient cells and their normal counterparts revealed that changes in GSH and GSSG per se do not cause cell death. These findings suggest that the failure of hepatoma cells to maintain energy metabolism in the midst of oxidative stress may cause cell death.

1. Introduction

Reactive oxygen species (ROS) are implicated in a number of physiological and pathophysiological processes. Depending on their level, ROS can serve as signaling molecules to promote cell proliferation or as mediator of cell death. Exposure to relatively high levels of oxidant induces apoptosis and necrosis. ROS inflict damages to cellular macromolecules, which, if not repaired, elicit apoptosis and necrosis [1, 2]. Normally, cells are equipped with an arsenal of antioxidants to impose a control on ROS generation [3, 4]. For instance, glutathione (GSH) acts as substrate for antioxidative enzymes. Glutathione peroxidase catalyzes reduction of hydroperoxides, accompanied by oxidation of GSH to its disulfide form. The latter is reduced back to GSH through the activity of glutathione reductase. NADPH is needed as a

coenzyme in the latter reaction. Inefficient NADPH production and GSH regeneration are known to promote death of cells under oxidative stress [5].

Maintenance of antioxidative defense depends on active metabolism. Oxidative stress rapidly increases the flux of glucose into the pentose phosphate pathway (PPP) and NADPH production. PPP activation is involved in cytoprotection against oxidative damage [6]. Consistent with this, glucose 6-phosphate dehydrogenase- (G6PD-) deficient cells are more susceptible to diamide-induced GSH depletion [5] and utilize different biochemical pathways in an attempt to maintain their GSH and NADPH pools [7, 8]. The GSH biosynthesis and NAD phosphorylation are upregulated at the cost of excessive energy usage. Moreover, the metabolic responses of erythrocytes to diamide differ from those of nucleated cells [7]. The interplay between oxidative stress,

the antioxidant system, and metabolism is more complicated than what has been previously thought. It is interesting to study if other oxidants, such as H_2O_2 , elicit metabolic responses unique from those of diamide treatment. Thorough understanding of metabolic changes in response to oxidants necessitates the application of metabolomics.

Intracellular NADPH/NADP⁺ and NADH/NAD⁺ are involved in maintenance of antioxidant defense and energy metabolism, respectively. Additionally, these pyridine nucleotides act as coenzymes in metabolism and have regulatory functions [9]. NAD⁺ is a precursor of cyclic ADP ribose [10] as well as a substrate for ADP ribosylation by poly-ADP-ribose polymerases (PARPs) [11], which are involved in processes such as DNA repair and cell death. The heightened PARP activation may activate programmed cell death despite antioxidant replenishment [12].

In this study, we used a LC-MS-based metabolomic research platform [8, 13] for studying the early changes in metabolite profile accompanying H_2O_2 -induced death. Our findings indicate that PPP is activated and production of S-1,7-BP, an unusual PPP intermediate, increases in H_2O_2 -treated cells. PPP and the NAD kinase (NADK) pathway are activated to furnish sufficient reducing equivalents. ATP and NAD⁺ pools dwindle, leading to dysfunction in metabolism. Inhibition of PARP-mediated exhaustion partially protects cells from death.

2. Material and Methods

2.1. Reagents. Unless otherwise stated, all chemicals were obtained from Sigma-Aldrich (St. Louis, MO, USA). Dulbecco's modified Eagle's medium (DMEM), fetal calf serum (FCS), penicillin, streptomycin, amphotericin, and trypan blue were purchased from Thermo Fisher Scientific Inc. (Waltham, MA, USA). Anti-G6PD antibody was purchased from Genesis Biotech (Taiwan); mouse anti-NADK monoclonal antibody (sc-100347) was available from Santa Cruz Biotechnology (CA, USA); rabbit anti-phospho-AMPK α (Thr172) (40H9) and rabbit anti-AMPK α (D5A2) antibodies were obtained from Cell Signaling Technology (Danvers, MA, USA). Anti-actin antibody and anti-rabbit and anti-mouse IgG antibodies were available from Sigma-Aldrich (St. Louis, MO, USA). Western Lightning Chemiluminescence Reagent Plus was purchased from PerkinElmer (Waltham, MA, USA).

2.2. Cell Culture and Cell Viability Determination. Hep G2 cells were cultured in DMEM supplemented with 10% FCS, 100 units/ml penicillin, 100 μ g/ml streptomycin, and 0.25 μ g/ml amphotericin at 37°C in a humidified atmosphere of 5% CO₂ as previously described [5].

Cell viability was determined using the neutral red uptake assay [5]. After H_2O_2 treatment, the cells in 24-well plates were incubated with 10% neutral red solution to a final concentration of 0.033% at 37°C for 2 h. Thereafter, the culture supernatant was removed, the cells were fixed in 0.1% CaCl₂, 0.5% formaldehyde, and the incorporated dye was solubilized in a 1% acetic acid, 50% ethanol solution. The absorbance

was measured using a microplate reader with a 540 nm test wavelength and a 690 nm reference wavelength.

2.3. Generation of G6PD-Knockdown and Scrambled Control Hep G2 Cells. The cassette for expressing G6PD and scrambled control shRNA has been described elsewhere [14]. It was subcloned in pSUPER.retro. puro vector (Oligoengine, Seattle, WA, USA). The retroviral vectors were packaged into amphotropic virus using PT67 cells, as previously described [5, 15]. Hep G2 cells were transduced with the packaged virus and selected for stable transfectants in a medium containing 3 μ g/ml puromycin.

2.4. Western Blotting Analysis. Western blotting was performed as previously described [5, 15]. Briefly stated, the cells were rinsed with cold PBS, scraped, and collected by centrifugation. They were immediately lysed in lysis buffer (20 mM Tris-HCl (pH 8), 1% Triton X-100, 137 mM NaCl, 1.5 mM MgCl₂, 10% glycerol, 1 mM EGTA, 1 mM NaF, 1 mM Na₃VO₄, 10 mM β -glycerophosphate, 1 mM phenylmethylsulfonyl fluoride, 1 μ g/ml leupeptin, and 1 μ g/ml aprotinin). Protein concentration of cell lysate was determined using the Bio-Rad protein assay kit (Bio-Rad Laboratories, Hercules, CA, USA). The sample was analyzed by SDS-PAGE and immunoblotting with anti-AMPK, anti-pAMPK, anti-NADK, and anti-actin antibodies.

2.5. Extraction of Cellular Metabolites. Extraction was performed as previously described with modifications [8, 16]. After removal of medium, cells were scraped in 80% methanol precooled at -80°C. The extract was collected, centrifuged at 14000 \times g for 15 min, and extracted once more with 80% methanol. The extracts were pooled and completely dried under nitrogen gas. The sample was dissolved in 200 μ l 0.1% formic acid, centrifuged at 14000 \times g for 15 min to remove debris, and subjected to LC-MS analysis.

2.6. LC-TOF-MS Analysis. Liquid chromatographic separation was achieved on a 100 mm \times 2.1 mm ACQUITY 1.8 μ m HSST3 C18 column (Waters Corp.; Milford, MA, USA) using an ACQUITY TM Ultra Performance Liquid Chromatography (UPLC) system (Waters). The column was maintained at 40°C, and the flow rate was set at 0.5 ml/min. Sample was eluted from LC column using a linear gradient: 0–1.5 min, 1–25% B; 1.5–2.0 min, 25–98% B; 2.0–4.9 min, 98% B; and 5.0–7.0 min, 1% B (for reequilibration). Solvent A was 0.1% formic acid in water and solvent B was acetonitrile containing 0.1% formic acid. The lyophilized sample was dissolved with 200 μ l of water/acetonitrile (95:5, v/v). Mass spectrometry was performed on a Waters Q Tof-MS (SYNAPT G2S, Waters MS Technologies, Manchester, UK) operated in an ESI negative ion mode. The scan range was from 50 to 990 m/z. The desolvation gas flow was set to 1000 l/hr at 500°C, and temperature was set at 150°C. The capillary voltage and cone voltage were set at 2000 and 25 V for the ESI negative mode. Leucine enkephalin, generating [M-H]⁻ ion (236.1035 m/z, 554.2615 m/z), was used as the lock mass at a concentration of 200 ng/ml and a flow rate of 10 μ l/min.

2.7. Data Processing. All data obtained in the negative ion mode were processed using Progenesis QI data analysis software (Nonlinear Dynamics, Newcastle, UK) for peak picking, alignment, and normalization to generate peak intensities for all features. The identities of features were obtained through search in METLIN (available at <https://metlin.scripps.edu>) [17] and Human Metabolome (available at <http://www.hmdb.ca/>) databases [18] and/or by comparison to both retention times and mass spectra of standard compounds. The MS data were analyzed by principal component analysis (PCA) and orthogonal partial least squares discriminate analysis (OPLS-DA) using SIMCA-P⁺ 13.0 (Umetrics, Sweden).

2.8. Metabolite Identification. For validation of the target metabolite, standards were analyzed under chromatographic conditions identical to that of the metabolite profiling experiment. MS and MS/MS analyses were performed under the same conditions as the metabolite profiling experiment. MS/MS spectra were collected at 0.3 second per scan, with a medium isolation window of ~ 4 m/z. The trap collision energy from 5 to 35 V was set.

3. Results

3.1. Distinct Impact of Hydrogen Peroxide on Global Metabolism of Hepatoma Cells. Our previous study has shown that GSH depletion significantly affects cellular metabolism and cell viability [8]. We sought to study if an oxidant can cause specific metabolic changes that are different from those brought about by GSH depletion. To test such possibility, we examined the changes in the metabolite profile of Hep G2 cells in response to H₂O₂ treatment. Hep G2 cells were treated without, or with 0.5 or 5 mM, H₂O₂ for a period ranging from 15 min to 2 hr. Cell extracts were analyzed using TOF-MS in negative ion mode. The experimental scheme is outlined in Supplemental Figure 1. The orthogonal partial least squares discriminate analysis (OPLS-DA) plot showed that the metabolite profile of cells treated with 5 mM H₂O₂ was significantly different from that of control cells. In contrast, there were mild changes in the metabolite profile of cells treated with 0.5 mM H₂O₂ versus that of control cells (Supplemental Figure 2B). Treatment of cells with 5 mM H₂O₂ for 4 hr resulted in considerable decline in viability, while treatment with 0.5 mM caused insignificant cell death (Supplemental Figure 2A).

To study the early metabolic changes associated with H₂O₂-induced cell death, we focused on the analysis of datasets for 5 mM H₂O₂ treatment and control groups. As shown in OPLS-DA (Figure 1(a)), there were time-dependent changes in metabolites in H₂O₂-treated cells. Significant changes in metabolites occurred as early as 15 min after treatment (Figure 1(b)). Those features with variable importance in the projection (VIP) score greater than 1 correspond to differentially abundant metabolites and were selected for further analysis (Figure 1(c) and Supplemental Table 1). Enrichment analysis revealed changes in metabolites related to the metabolism of nucleotide, citric acid, glutamate, glucose, glutathione, and ammonia cycle in cells (Figure 1(d)).

These findings suggest that these pathways may represent the early cellular metabolic response to H₂O₂-induced death.

3.2. H₂O₂-Induced Accumulation of S-1,7-BP and Fru-1,6-BP. Of the metabolites that changes in H₂O₂-treated cells, several metabolites related to the nonoxidative pentose phosphate pathway (PPP) are noteworthy. Fructose 1,6-bisphosphate (Fru-1,6-BP), the metabolite involved in regeneration of glucose, accumulated over time (Figure 2(a)). Intriguingly, the S-1,7-BP level rapidly increased by nearly 11.41-fold within 15 min of treatment, peaked at 30 min, and subsided (Figure 2(b); Supplemental Table 1). The identities of Fru-1,6-BP (Figure 2(c) & 2(d)) and S-1,7-BP (Figure 2(e)) were validated by MS/MS. Similarly, octulose-1,8-bisphosphate (O-1,8-BP) increased by roughly 6.75-fold at 15 min after treatment, remained elevated up to 60 min, and gradually declined afterwards (Supplemental Table 1). Previous studies have shown that S-1,7-BP and O-1,8-BP were present in hemolysate and thought to be synthesized by aldolase in a distinct type of nonoxidative PPP [19–21]. Our recent findings suggest that PPP is activated in response to treatment with high H₂O₂ concentration.

3.3. H₂O₂-Induced Changes in Redox and Energy Metabolism. GSH metabolism is affected by H₂O₂ treatment. The GSSG level increased to nearly 5 times the basal level within 30 min of treatment and stayed more or less steady throughout the treatment period. The decline in the GSH level was relatively modest during the same period (Supplemental Table 1). Such findings suggest that GSH buffer is largely maintained. However, other GSH-related intermediates were affected. For instance, the S-lactoylglutathione level increased over 130-fold within 90 min of treatment and declined afterwards (Supplemental Table 1).

Energy metabolism was drastically affected. Levels of nucleoside triphosphate, such as ATP and CTP, were drastically reduced, whereas monophosphate forms AMP, UMP, and GMP strongly increased in abundance. Moreover, cellular NAD⁺ decreased appreciably during H₂O₂ treatment (Supplemental Table 1). Besides, citrate accumulated over time during treatment. Apparently, cellular energy metabolism is adversely affected in the presence of high H₂O₂ concentration.

3.4. Knockdown of G6PD Impairs PPP and GSH Metabolism. Diamide that induces mild changes in cellular GSH and GSSG in normal hepatoma cells does not significantly affect their viability [8]. In contrast, treatment with 5 mM H₂O₂, which caused similar changes in the abundance of GSH and GSSG as diamide, elicited cell death. It is wondered that redox parameters, such as GSSG/GSH redox potential, are not the sole determinant of the cellular outcome of H₂O₂ treatment. G6PD is critical to maintenance of NADPH and GSH. We studied the effect of G6PD knockdown on H₂O₂-induced changes in metabolism and cell physiology. We knocked down expression of *G6PD* gene in Hep G2 cells and derived knockdown (Gi) and control (Sc) cells. As expected, the G6PD activity in Gi cells was reduced by 90%, as compared with that in Sc cells (Figure 3(a)). H₂O₂

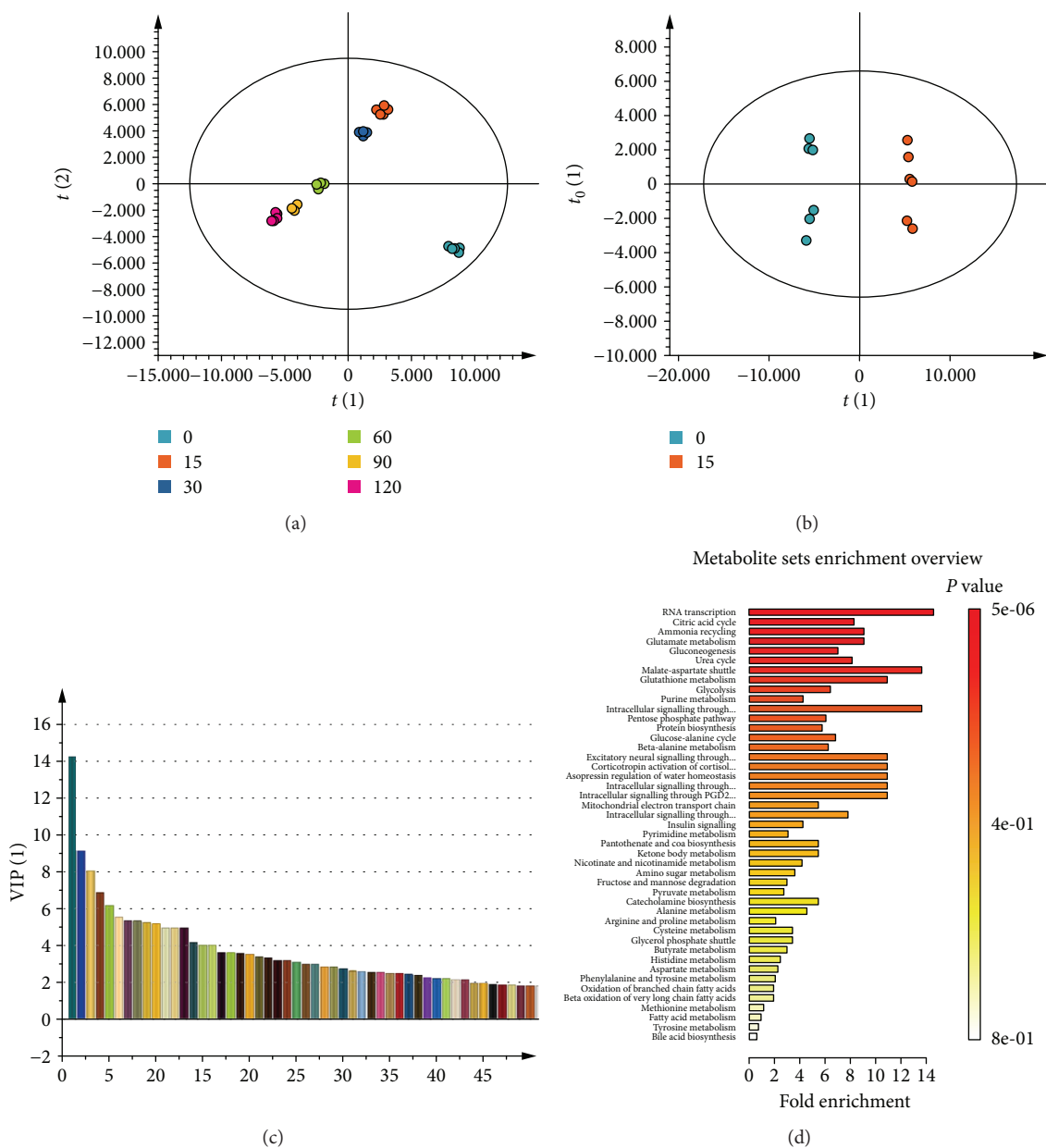


FIGURE 1: Early changes in metabolism of H_2O_2 -treated hepatoma cells. Cells were treated with 5 mM H_2O_2 for 0, 15, 30, 60, 90, and 120 min and harvested for metabolomic analysis. Molecular features were identified by Progenesis Q1, and the data were processed and analyzed using SIMCA-P. (a) Orthogonal partial least squares discriminant analysis (OPLS-DA) score plot for various treatment groups are shown. (b) OPLS-DA score plot of the 0 min- and 15 min-treated groups. The ellipse shown in the model (a, b) represents the Hotelling's T^2 with 95% confidence. (c) Variable importance in projection (VIP) plot of the OPLS-DA model for the 0 min- and 15 min-treated groups. Selected metabolites with a VIP value > 1.0 are presented. (d) The data were subjected to metabolite pathway analysis. A summary plot for metabolite set enrichment analysis (MSEA), in which metabolite sets are ranked according to the p value, is shown. The bar plot is color coded according to the calculated p values.

treatment induced a slightly higher degree of cell death in Gi cells than in Sc cells (Figure 3(b)). To examine the effect of H_2O_2 on metabolism, we treated Gi and Sc cells with 5 mM H_2O_2 for 15, 30, 60, 90, and 120 min and extracted them for metabolite profiling. Datasets were analyzed using multivariate statistical analyses. The OPLS-DA plots for Gi and Sc cells are shown in Figure 3(c). The metabolite profile of these cells changed in a time-dependent manner. As expected, PPP is adversely affected by G6PD deficiency

(Figure 4). The levels of PPP intermediates, such as sedoheptulose 7-phosphate (S7P), 6-phosphoglucono- δ -lactone, 6-phosphogluconate (6PG), and ribulose 5-phosphate, in Gi cells were significantly lower than those in Sc cells. Additionally, the S-1,7-BP level was largely lowered in Gi cells, advocating that S-1,7-BP is an intermediate formed in the nonoxidative branch of PPP.

Temporal changes in GSH and GSSG were also followed (Figure 4). The levels of GSSG in Gi and Sc cells increased

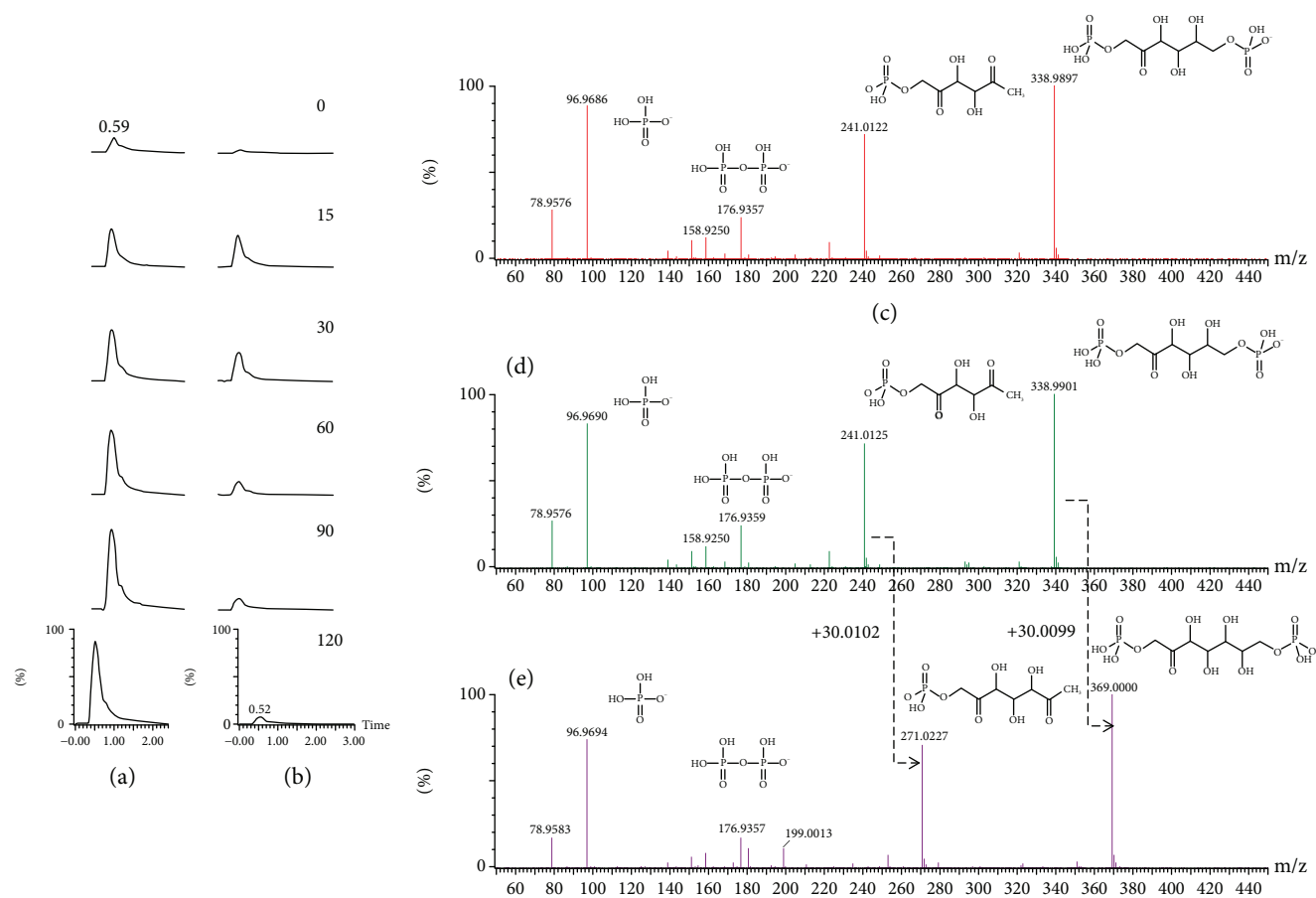


FIGURE 2: Oxidative stress-induced accumulation of Fru-1,6-BP and S-1,7-BP. The extracted ion chromatograms of Fru-1,6-BP (a) and S-1,7-BP (b) in Hep G2 cell treated with 5 mM H_2O_2 for 0, 15, 30, 60, 90, and 120 min are shown. Metabolite abundance is indicated by the peak intensity. A representative experiment is shown. The identities of Fru-1,6-BP (c, d) and S-1,7-BP (e) were validated by MS/MS analysis. The MS/MS spectrum of Fru-1,6-BP in cell specimen (d) was matched against that of standard (c). The spectrum of S-1,7-BP reveals a parent cation (369.0001 m/z) and a fragment ion (271.0227 m/z). The latter differs from the fragment ion of Fru-1,6-BP (241.0125 m/z) by a CHOH unit (30.01 m/z). For (c–e), the chemical structures of the fragment ions and their experimentally obtained m/z values are shown alongside the corresponding peaks.

within 30 min of treatment and were significantly lowered at 60 min after treatment. The extent of the surge in the GSSG level was much higher in the former than in the latter. The basal GSH level in Gi cells was higher than that in Sc cells. Upon H_2O_2 treatment, the GSH level in Gi cells showed a transient large drop and gradually stabilized at a value lower than the basal level. Meanwhile, the GSH abundance in Sc cells declined gradually with time and was not significantly different from that in Gi cells at 120 min. Apparently, the dynamic changes in the GSSG and GSH pools in these cells, particularly Gi cells, represent their effort to restore GSH homeostasis. Notwithstanding the differences in the kinetics and extent of changes in GSH and GSSG levels between Gi and Sc cells, H_2O_2 treatment results in the same outcome—cell death. These findings, together with our previous studies on diamide, indicate that changes in GSH and GSSG levels per se do not determine the fate of cells exposed to high concentration of H_2O_2 . It is likely that events consequent to changes in redox homeostasis may be linked to initiation of H_2O_2 -induced cell death.

3.5. H_2O_2 Treatment Causes Anomalous Energy Metabolism. Our previous study has shown that energy metabolism is hampered in diamide-treated cells [8]. As shown in Supplemental Table 1, ATP was significantly reduced in H_2O_2 -treated cells. We proceeded to examine the changes in levels of ATP in Gi and Sc cells receiving H_2O_2 treatment. ATP levels in Gi and Sc cells declined dramatically with treatment time (Figure 5(a)). Basal ADP and AMP levels in Sc were substantially lower than those in Gi cells. The ADP levels of Sc and Gi cells increased, peaked at 15 min, and declined thereafter (Figure 5(b)). The AMP levels of Sc and Gi cells spiked at 15 min and returned to values higher than their basal levels (Figure 5(c)). Accumulation of AMP was associated with phosphorylation of AMPK at Thr172 (Figure 5(f)). These findings suggest that H_2O_2 induces ATP depletion. As treatment of Sc and Gi cells with 0.5 mM H_2O_2 did not cause their death, we examined the effect of 0.5 mM H_2O_2 on the cellular ATP content. As shown in Figure 6(a), in contrast to 5 mM H_2O_2 , 0.5 mM H_2O_2 induced a significant increase in the ATP level over time.

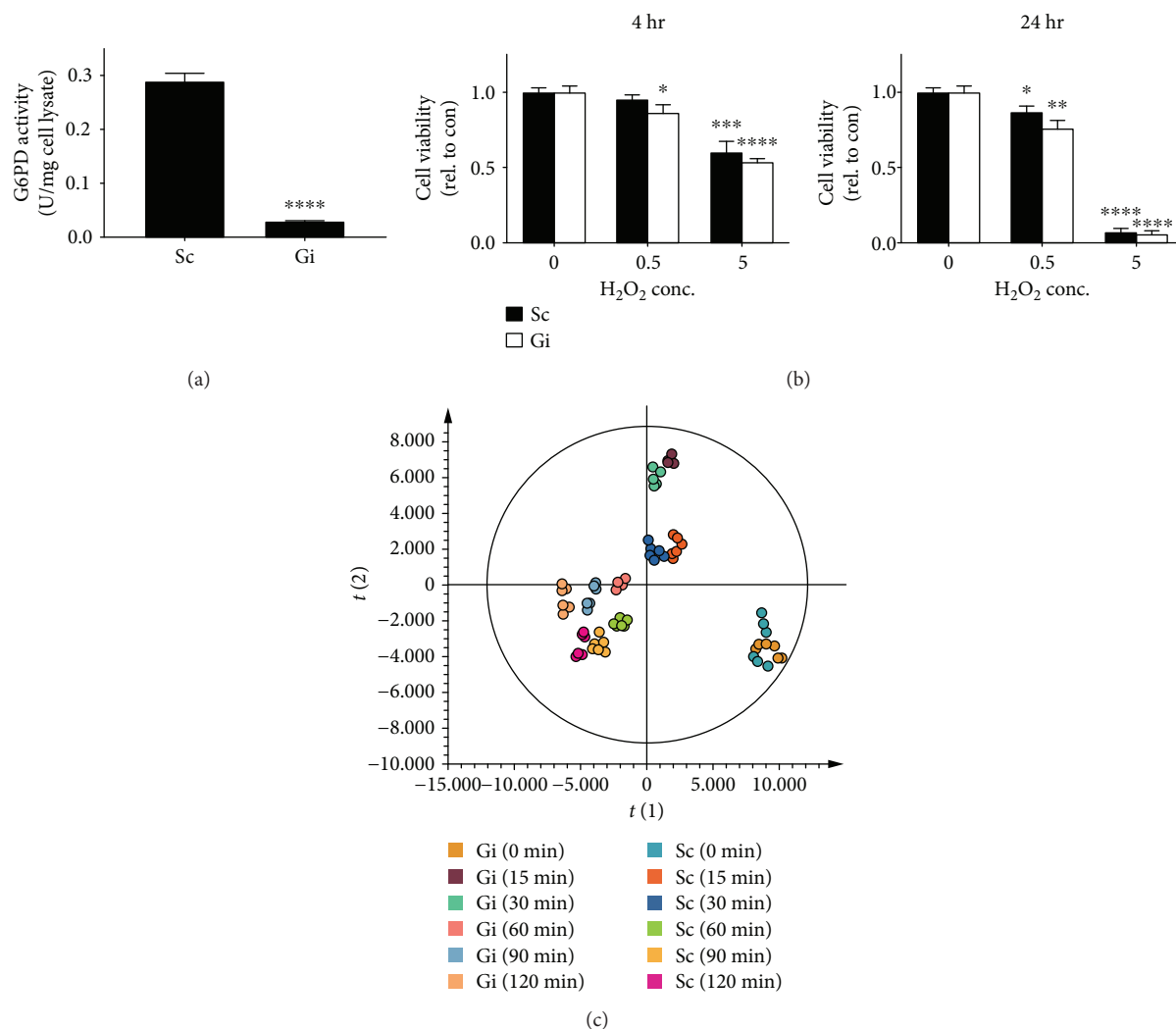


FIGURE 3: Temporal changes in metabolism in G6PD-deficient hepatoma cells. (a) G6PD activities in Sc and Gi cells were measured and are expressed in U/mg of cell lysate. Data are means \pm SD, $n = 6$. (b) Sc and Gi cells were untreated or treated with 0.5 and 5 mM H₂O₂ for 4 and 24 hr, and their viabilities were determined. Data are means \pm SD, $n = 6$. (c) Sc and Gi cells were treated with 5 mM H₂O₂ for 0, 15, 30, 60, 90, and 120 min and collected for metabolomic analysis. Data were analyzed as described in the legend of Figure 1. The OPLS-DA score plot of Sc and Gi cells treated for various times is shown.

3.6. H₂O₂ Treatment Induces Expression of NADK and Biosynthesis of NADP⁺. The transient increase in GSSG in Gi cells prompts us to study if pathways other than PPP provide reducing equivalents for its reduction. It is probable that NADP⁺ synthesis is upregulated during H₂O₂ treatment. Consistent with this, the NADP⁺ level in Gi and Sc cells increased substantially within 30 min of treatment. The magnitude of the increase was significantly greater in the former than in the latter (Figure 5(e)). The basal NAD⁺ level in Gi cells was lower than that in Sc cells. Upon H₂O₂ treatment, it decreased drastically (Figure 5(d)).

NADK, which catalyzes NAD⁺ phosphorylation and its conversion to NADP⁺, may be part of the compensatory mechanism. To study whether NADK is involved, we examined NADK expression in H₂O₂-treated Sc and Gi cells. As shown in Figure 5(f), expression of NADK increased in both cells, with the induction fold being higher in Gi cells than in Sc cells.

3.7. Inhibition of PARP-Mediated NAD⁺ Depletion Partially Protects Cells from Death. H₂O₂ treatment causes NAD⁺ depletion. There were large drops in the NAD⁺ level in Gi and Sc cells within 15 min of treatment with either 0.5 or 5 mM H₂O₂ (Figure 6(b)). For the 5 mM treatment group, their NAD⁺ levels continued to decline from 15 min onward. In contrast, for the 0.5 mM treatment group, the NAD⁺ levels of Gi and Sc cells stabilized at 15 min posttreatment and gradually rebounded to values that were about 30% of their respective basal levels.

One of the routes, through which NAD⁺ is rapidly utilized and exhausted, is poly (ADP-ribose) polymerase (PARP). ROS are known to cause single-strand breaks and PARP activation [22]. To test if PARP-mediated depletion of NAD⁺ accounts for cell death, we cotreated Hep G2 cells with PARP inhibitor PJ34 and H₂O₂ and examined their viability. Treatment of Hep G2 cells with PJ34 enhanced viability but did not completely block their death (Figure 7). These

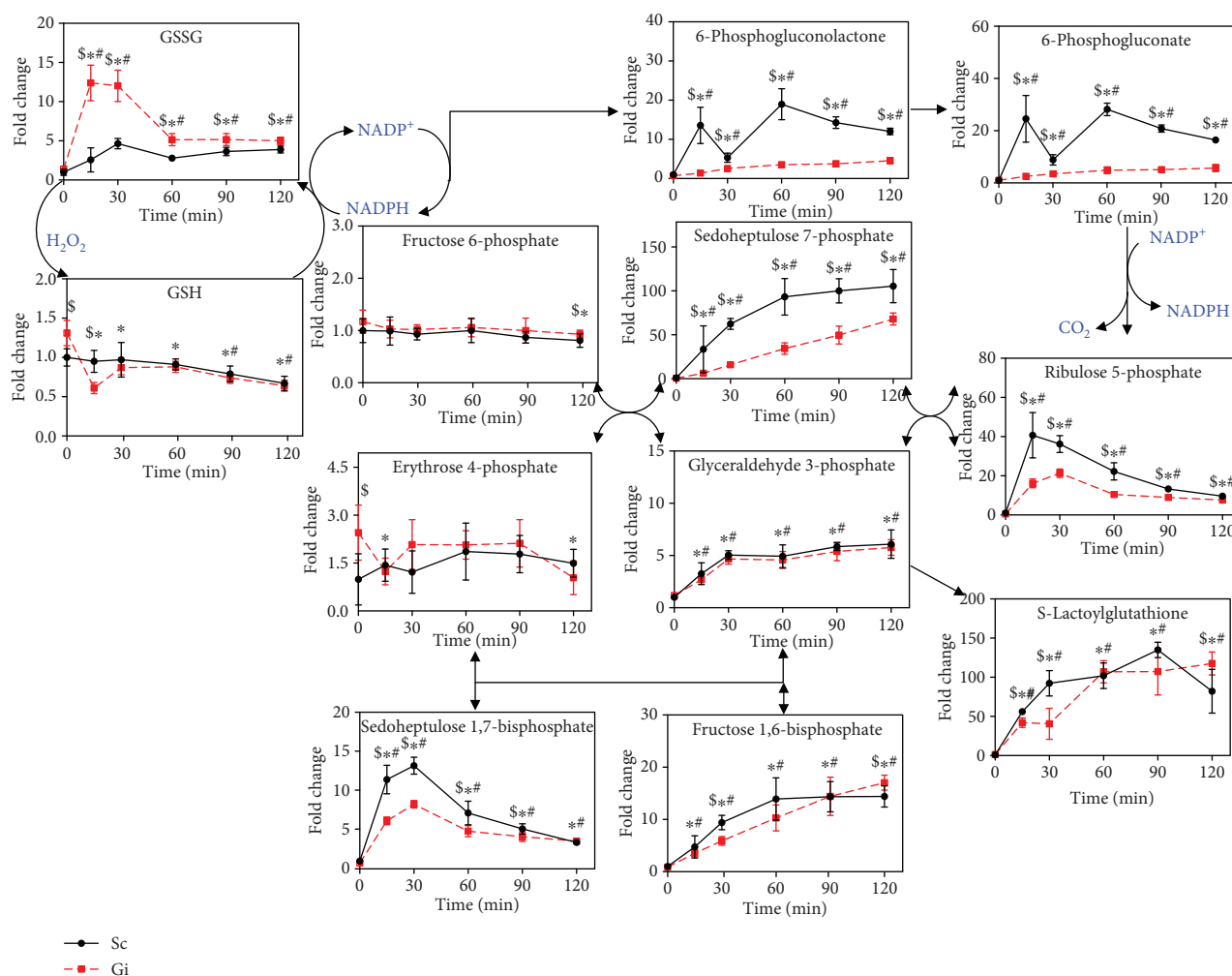


FIGURE 4: Changes in intermediates in PPP and glutathione metabolism. Analysis of metabolomic data that were obtained as described in the legend of Figure 3(c) reveals that a number of metabolites in PPP and glutathione metabolism change with time after H_2O_2 treatment. The levels of metabolites are expressed relative to that of untreated Sc cells. Data are means \pm SD, $n = 6$. $^{\$}p < 0.05$, Sc cells vs Gi cells; $^{\#}p < 0.05$, treated vs untreated Gi cells; and $^*p < 0.05$, treated vs untreated Sc cells.

findings suggest that PARP-mediated NAD^+ depletion contributes partly to the death process.

4. Discussion

In this study, we have applied the metabolomic approach for studying the metabolic response of hepatoma cells to H_2O_2 . High concentration of H_2O_2 significantly alters the fluxes of metabolic pathways. Some of these pathways, such as the PPP and NADK pathway, are activated to restore redox homeostasis. Despite their effectiveness, these pathways lead to excessive consumption of NAD^+ and ATP. Our findings support the notion that impairment of energy metabolism precipitates cell death.

H_2O_2 -induced changes in metabolism are different from what we observed in diamide-treated cells. Diamide reacts with thiols and causes GSH depletion. It induces time-dependent changes in metabolic pathways, such as GSH biosynthesis, amino acid metabolism, and energy metabolism, in hepatoma cells [8]. GSH biosynthesis and

amino acid uptake are not enhanced in H_2O_2 -treated cells. The disparity may lie in the fact that diamide is highly effective in the conversion of GSH to GSSG and hence GSH pool diminution. This may lead to the relief of the inhibitory effect of GSH on glutamate cysteine ligase (GCL) [23] and to the subsequent γ -glutamylcysteine formation. In agreement with this, diamide is superior to H_2O_2 in its ability to deplete the cellular GSH pool [24]. Nonetheless, there are metabolic changes commonly induced by H_2O_2 and diamide. For instance, energy metabolism is adversely affected [8]. PPP is important to the provision of reducing equivalents [7].

PPP is activated in response to oxidant treatment. Levels of intermediates of normal PPP, such as sedoheptulose 1,7-bisphosphate and ribulose 5-phosphate, increased with treatment time. We detected metabolites that are supposedly to be formed in the L-type pathway [25]. These metabolites include S-1,7-BP and O-1,8-BP. S-1,7-BP has been found in erythrocytes and liver tissues. It is conjectured that S-1,7-BP can be formed from dihydroxyacetone phosphate and erythrose-4-phosphate (E4P) via aldolase activity. E4P

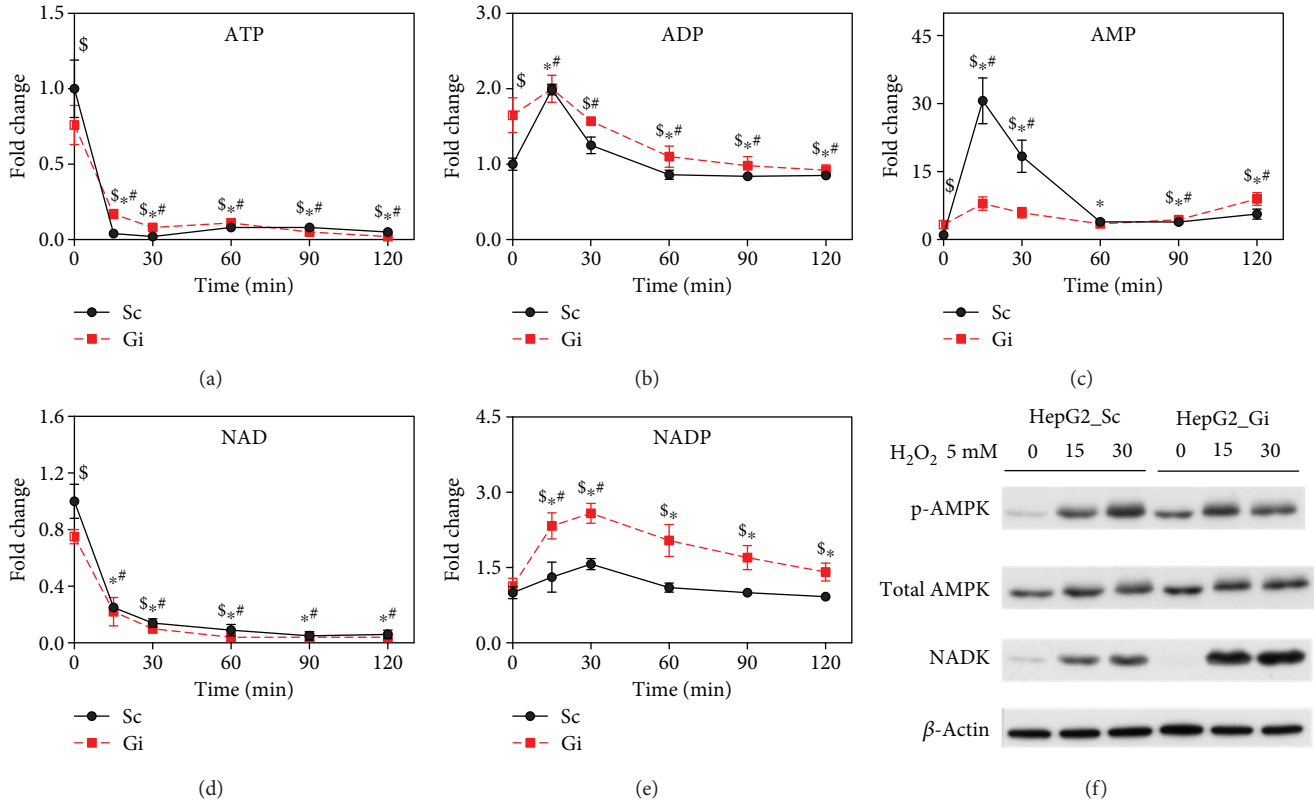


FIGURE 5: Oxidative stress-induced changes in energy and redox metabolism. Sc and Gi cells were treated with 5 mM H_2O_2 for 0, 15, 30, 60, 90, and 120 min. The cells were harvested, and cellular levels of ATP (a), ADP (b), AMP (c), NAD^+ (d), and $NADP^+$ (e) were determined by LC-MS. The levels of metabolites are expressed relative to those of untreated Sc cells. Data are means \pm SD, $n = 6$. (f) Sc and Gi cells were untreated or treated with 5 mM H_2O_2 for 0, 15, and 30 min and harvested for immunoblotting with antibodies to p-AMPK, AMPK, NADK, and actin. A representative experiment out of three is shown. $\$p < 0.05$, Sc cells vs Gi cells; $*p < 0.05$, treated vs untreated Gi cells; and $\#p < 0.05$, treated vs untreated Sc cells.

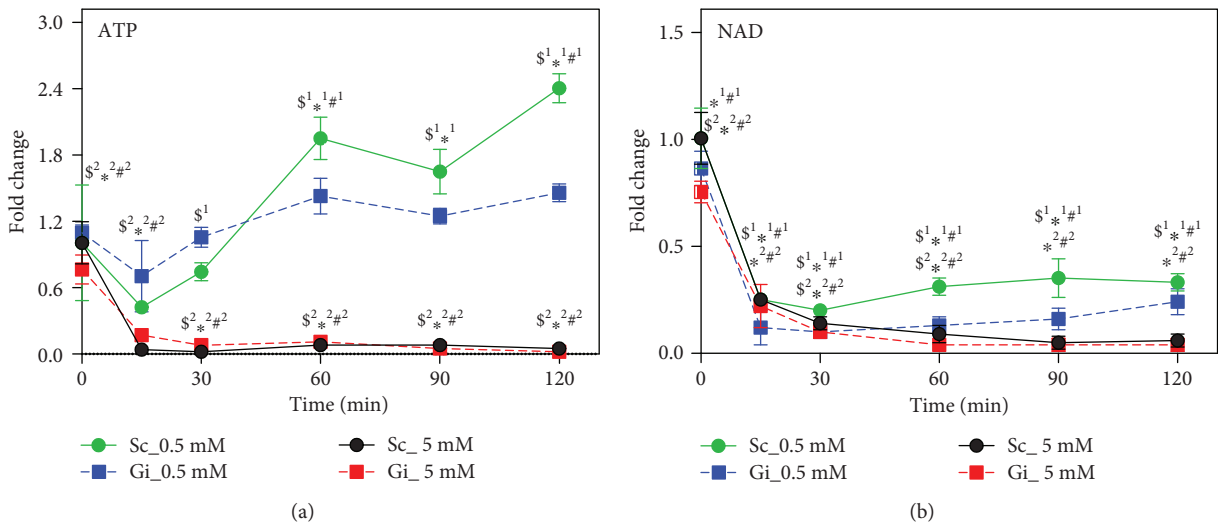


FIGURE 6: ATP and NAD exhaustion accounts for death of hepatoma cells subject to oxidative stress. Sc and Gi cells were treated with 0.5 or 5 mM H_2O_2 for 0, 15, 30, 60, 90, and 120 min and were extracted for LC-MS analysis of ATP (a) and NAD^+ (b). The levels of metabolites are expressed relative to that of untreated Sc cells. Data are means \pm SD, $n = 6$. $\$^1p < 0.05$ or $\$^2p < 0.05$, Sc cells vs Gi cells treated with 0.5 mM or 5 mM H_2O_2 ; $\#^1p < 0.05$ or $\#^2p < 0.05$, treated vs untreated Gi cells upon treatment with 0.5 mM or 5 mM H_2O_2 ; and $\#^1p < 0.05$ or $\#^2p < 0.05$, treated vs untreated Sc cells upon treatment with 0.5 mM or 5 mM H_2O_2 .

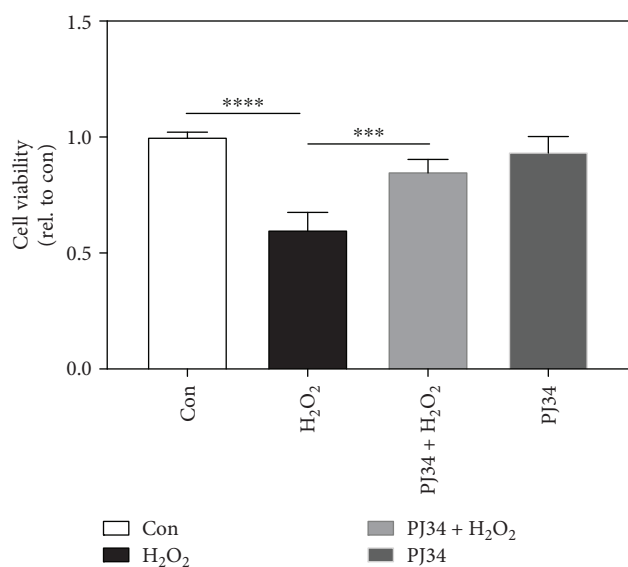


FIGURE 7: Inhibition of PARP partially rescues hepatoma cells from death. Hep G2 cells were pretreated with 30 μ M PJ34 for 2 hr prior to treatment with 5 mM H₂O₂. Cell viability was determined and is expressed relative to control. Data are means \pm SD, $n = 6$. *** $p < 0.005$ and **** $p < 0.001$.

can replace glyceraldehyde-3-phosphate (G3P) as a substrate for S-1,7-BP synthesis in extracts of mammalian tissues such as the liver and muscle [21, 26]. Additionally, it may be formed from fructose 1,6-bisphosphate and E4P. Alternatively, 6-phosphofructokinase may catalyze S-1,7-BP formation from sedoheptulose 7-phosphate. O-1,8-BP may arise from condensation of DHAP and ribose 5-phosphate [27]. In our present study, we validate that these metabolites are formed in nonoxidative PPP. Knockdown of the *G6PD* gene significantly reduced the levels of these metabolites. In this sense, S-1,7-BP is considered a marker of increased PPP activity.

Our previous study has shown that diamide treatment caused about 11% decrease in the GSH pool in hepatoma cells at 60 min posttreatment [8]. In the present study, H₂O₂ treatment resulted in around a 10% decrease in this pool. Despite the similarity in the extent of change, H₂O₂ induced cell death, while diamide did not. Such findings suggest that factors other than simply a change in GSH parameter contribute to cell death.

H₂O₂ treatment causes anomalous energy production. The ATP level decreased continually throughout treatment and became virtually exhausted. ADP and AMP levels transiently rose and gradually subsided. The increases in ADP and AMP levels activate AMPK and cause influx of glucose into the glycolytic pathway. The increase in glycolytic flux is indicated by increases in levels of fructose 1,6-bisphosphate and glyceraldehyde 3-phosphate. Additionally, such increases may promote the nonoxidative branch of PPP for glucose regeneration and continual operation of PPP. Furthermore, accumulation of glyceraldehyde 3-phosphate is accompanied by formation of lactoylglutathione. Lactoylglutathione is derived from methylglyoxal and glutathione via the activity of glyoxalase I [28, 29]. This represents a pathway

involved in detoxification of methylglyoxal, which is able to glycate nucleic acid and protein and conduces to advanced glycation end product (AGE) formation [30]. Methylglyoxal is formed either nonenzymatically from dihydroxyacetone phosphate and glyceraldehyde 3-phosphate or enzymatically via a triosephosphate isomerase-mediated process [28]. It has been demonstrated that a low NAD⁺ level promotes generation of methylglyoxal [31]. H₂O₂-induced deficit in NAD⁺ probably reduces the flux of glyceraldehyde 3-phosphate-catalyzed reaction and makes it favorable for diversion of triose phosphate toward methylglyoxal formation. An additional point is noteworthy. The total pool of adenine nucleotides dwindles, suggesting their transformation to other molecules. We observed that the level of diadenosine diphosphate spiked within the first 30 min of H₂O₂ treatment and remained elevated. Diadenosine diphosphate (Ap₂A) is formed in a side reaction catalyzed by aminoacyl tRNA synthetase in the absence of cognate tRNA [32]. Diadenosine oligophosphate is proposed as a novel class of signaling molecules. For instance, Ap₃A binds to the Fhit protein and, as a complex, serves as effector molecule with tumor suppressor activity [33]. Ap_nA interacts with P2Y and P2X receptors and elicits downstream signaling [34]. Ap₂A protects neutrophils from apoptosis [35]. In addition, Ap₂A stimulates growth of vascular smooth muscle cells [36]. It is probable that Ap₂A might be generated in H₂O₂-treated cells in an attempt to rescue them from demise. Moreover, another metabolite adenylosuccinate increased in abundance within 15 min of treatment and gradually declined. It is an intermediate formed in the path of conversion of IMP to AMP. H₂O₂-induced change in the adenylosuccinate pool probably represents a biochemical response of cells in the face of ATP depletion. These cells upregulate purine biosynthesis to make up for the deficit.

AMPK is composed of 3 subunits, including catalytic α subunit and regulatory β and γ subunits. It acts as an important energy sensor molecule that controls cellular physiology [37, 38]. AMPK is activated by an increase in the AMP/ATP ratio under the stressful condition that hinders ATP generation and accelerates its consumption [39]. Its activity can also be modulated by ADP and NAD⁺ [40–42]. Moreover, AMPK can be regulated indirectly through reactive nitrogen species-mediated activation of upstream kinases LKB1 and CaMKKb or through S-glutathionylation or S-nitrosylation of cysteine residues of the AMPK α subunit [43, 44]. H₂O₂-induced increases in AMP and ADP, and probably oxidative modification, activate AMPK. AMPK activation enhances hepatic glucose uptake via Glut2 [45]. AMPK is able to phosphorylate phosphofructokinase 2 [46], which generates fructose 2,6-bisphosphate, a potent activator of phosphofructokinase 1. Increase in fructose 1,6-bisphosphate in H₂O₂-treated cells may be accounted for by an increased flux of phosphofructokinase 1-catalyzed reaction.

H₂O₂-induced changes in nicotinamide adenine nucleotide pools have important implication in biochemical and cellular processes. NAD⁺ depletion, amid the maintenance of the NADP⁺ pool, is associated with increased NADK expression. Menadione increases NADK activity and causes NAD⁺ depletion in colon epithelial cells [47]. NADK activity

increases in diamide-treated G6PD-deficient cells [8]. It is plausible that upregulation of NADK represents a mechanism for maintenance of the NADP⁺ pool [48, 49]. Mammalian NADK catalyzes formation of NADP⁺ at the expense of NAD⁺ and ATP. Increased NADK activity in H₂O₂-treated cells, particularly Gi cells, contributes to diminution of the NAD⁺ and ATP pools. Oxidative damage-induced DNA damage leads to activation of poly (ADP ribose) polymerase (PARP) and NAD⁺ depletion [50, 51]. Treatment with the PARP inhibitor partially protects H₂O₂-treated cells from death, implying that activation of PARP is involved in cell death. These findings suggest that depletion of NAD⁺ and ATP can trigger cell death. Deficit in NAD⁺ leads to reduction in glycolysis and oxidative phosphorylation and hence to insufficient ATP production. When NAD⁺ and ATP levels fall below certain thresholds, cells are destined to die.

Accumulation of citrate in H₂O₂-treated cells is interesting. H₂O₂ increases the intracellular glutamine level and concomitantly reduces the glutamate level. Glutamine is available in culture medium as energy source and is converted to glutamate by glutaminase. Glutamate can be catabolized to α -ketoglutarate via action of glutamate dehydrogenase. α -Ketoglutarate is metabolized via forward reactions of the TCA cycle or transformed via isocitrate dehydrogenase and aconitase to citrate in a process known as reductive carboxylation. For the former process, citrate abundance is elevated as a consequence of reduced mitochondrial aconitase activity. Aconitase is uniquely sensitive to superoxide-mediated inactivation [52, 53]. Another nonexclusive possibility is that reductive carboxylation is essential to the maintenance of redox balance [54] and is probably upregulated as a response to oxidative stress. Citrate formed by reductive carboxylation is transported to the cytoplasm, where it is acted upon by cytosolic aconitase and isocitrate dehydrogenase to generate NADPH. H₂O₂-induced citrate accumulation may represent such an antioxidative mechanism.

A number of mechanisms come into play to maintain redox homeostasis. Activation of PPP protects cells from oxidative damage within the first few minutes of treatment [6]. Reductive carboxylation and NADK may provide an additional supportive role for NADPH generation. PARP activation is involved in signaling of the DNA repair process. These antioxidative and repair mechanisms may be activated in cells subject to oxidative stress and consume NAD⁺ and ATP. In milieu of strong oxidative stress, excessive utilization of these key metabolites leads to cellular energy stress and cell death.

Data Availability

The metabolic and oxidative data used to support the findings of this study are available from the corresponding author upon request.

Conflicts of Interest

The authors declare no conflict of interest.

Acknowledgments

The research work was supported, in whole or in part, by grants from Chang Gung Memorial Hospital (BMRP819, BMRP564, CMRPD1F0471, CMRPD1F0472, CMRPD1F0473, CMRPD1H0201, CMRPD1F0511, CMRPD1F0512, and CMRPD1F0513), the Ministry of Science and Technology, Taiwan (MOST 104-2320-B-182-022-MY3, MOST 107-2320-B-182-011-MY3, MOST 104-2320-B-182-017-MY3, MOST 107-2320-B-182-030, and MOST 107-3017-F-182-001), and the Ministry of Education (MOE) in Taiwan (EMRPD1G0251, EMRPD1H0401).

Supplementary Materials

Supplemental Table 1: a list of metabolites differentially abundant in the 0 min- versus 15 min-treated groups. Supplemental Figure 1: the workflow of our experiment. Supplemental Figure 2: temporal changes in metabolism in H₂O₂-treated Hep G2 cells. (*Supplementary Materials*)

References

- [1] S. V. Avery, "Molecular targets of oxidative stress," *Biochemical Journal*, vol. 434, no. 2, pp. 201–210, 2011.
- [2] N. Kaplowitz, "Mechanisms of liver cell injury," *Journal of Hepatology*, vol. 32, 1 Supplement, pp. 39–47, 2000.
- [3] C. Munoz-Pinedo, N. El Mjiyad, and J. E. Ricci, "Cancer metabolism: current perspectives and future directions," *Cell Death & Disease*, vol. 3, no. 1, p. e248, 2012.
- [4] R. A. Cairns, I. S. Harris, and T. W. Mak, "Regulation of cancer cell metabolism," *Nature Reviews Cancer*, vol. 11, no. 2, pp. 85–95, 2011.
- [5] L. P. Gao, M. L. Cheng, H. J. Chou, Y. H. Yang, H. Y. Ho, and D. Tsun-Yee Chiu, "Ineffective GSH regeneration enhances G6PD-knockdown Hep G2 cell sensitivity to diamide-induced oxidative damage," *Free Radical Biology & Medicine*, vol. 47, no. 5, pp. 529–535, 2009.
- [6] A. Kuehne, H. Emmert, J. Soehle et al., "Acute activation of oxidative pentose phosphate pathway as first-line response to oxidative stress in human skin cells," *Molecular Cell*, vol. 59, no. 3, pp. 359–371, 2015.
- [7] H. Y. Tang, H. Y. Ho, P. R. Wu et al., "Inability to maintain GSH pool in G6PD-deficient red cells causes futile AMPK activation and irreversible metabolic disturbance," *Antioxidants & Redox Signaling*, vol. 22, no. 9, pp. 744–759, 2015.
- [8] H. Y. Ho, M. L. Cheng, M. S. Shiao, and D. T. Y. Chiu, "Characterization of global metabolic responses of glucose-6-phosphate dehydrogenase-deficient hepatoma cells to diamide-induced oxidative stress," *Free Radical Biology and Medicine*, vol. 54, pp. 71–84, 2013.
- [9] R. H. Houtkooper, C. Canto, R. J. Wanders, and J. Auwerx, "The secret life of NAD⁺: an old metabolite controlling new metabolic signaling pathways," *Endocrine Reviews*, vol. 31, no. 2, pp. 194–223, 2010.
- [10] H. C. Lee, "Structure and enzymatic functions of human CD38," *Molecular Medicine*, vol. 12, no. 11–12, pp. 317–323, 2006.

- [11] S. Messner and M. O. Hottiger, "Histone ADP-ribosylation in DNA repair, replication and transcription," *Trends in Cell Biology*, vol. 21, no. 9, pp. 534–542, 2011.
- [12] Y. Zhu, K. K. Zhao, Y. Tong et al., "Exogenous NAD⁺ decreases oxidative stress and protects H₂O₂-treated RPE cells against necrotic death through the up-regulation of autophagy," *Scientific Reports*, vol. 6, no. 1, p. 26322, 2016.
- [13] M. L. Cheng, M. S. Shiao, D. T. Y. Chiu, S. F. Weng, H. Y. Tang, and H. Y. Ho, "Biochemical disorders associated with antiproliferative effect of dehydroepiandrosterone in hepatoma cells as revealed by LC-based metabolomics," *Biochemical Pharmacology*, vol. 82, no. 11, pp. 1549–1561, 2011.
- [14] H. Y. Ho, M. L. Cheng, Y. H. Wang, and D. T. Y. Chiu, "Flow cytometry for assessment of the efficacy of siRNA," *Cytometry Part A: The Journal of the International Society for Analytical Cytology*, vol. 69A, no. 10, pp. 1054–1061, 2006.
- [15] C. J. Lin, H. Y. Ho, M. L. Cheng, T. H. Cheng, J. S. Yu, and D. T. Y. Chiu, "Impaired dephosphorylation renders G6PD-knockdown HepG2 cells more susceptible to H₂O₂-induced apoptosis," *Free Radical Biology and Medicine*, vol. 49, no. 3, pp. 361–373, 2010.
- [16] A. D. Patterson, H. Li, G. S. Eichler et al., "UPLC-ESI-TOFMS-based metabolomics and gene expression dynamics inspector self-organizing metabolomic maps as tools for understanding the cellular response to ionizing radiation," *Analytical Chemistry*, vol. 80, no. 3, pp. 665–674, 2008.
- [17] R. Tautenhahn, K. Cho, W. Uritboonthai, Z. Zhu, G. J. Patti, and G. Siuzdak, "An accelerated workflow for untargeted metabolomics using the METLIN database," *Nature Biotechnology*, vol. 30, no. 9, pp. 826–828, 2012.
- [18] D. S. Wishart, T. Jewison, A. C. Guo et al., "HMDB 3.0—the human metabolome database in 2013," *Nucleic Acids Research*, vol. 41, no. D1, pp. D801–D807, 2013.
- [19] L. M. McIntyre, D. R. Thorburn, W. A. Bubb, and P. W. Kuchel, "Comparison of computer simulations of the F-type and L-type non-oxidative hexose monophosphate shunts with 31P-NMR experimental data from human erythrocytes," *European Journal of Biochemistry*, vol. 180, no. 2, pp. 399–420, 1989.
- [20] K. K. Arora, J. P. Longenecker, and J. F. Williams, "Mechanism and quantitative contribution of the pentose pathway to the glucose metabolism of Morris hepatoma 5123C," *International Journal of Biochemistry*, vol. 19, no. 2, pp. 133–146, 1987.
- [21] I. A. Rose and J. V. B. Warms, "Complexes of muscle aldolase in equilibrium with fructose 1,6-bisphosphate," *Biochemistry*, vol. 24, no. 15, pp. 3952–3957, 1985.
- [22] C. Nosseri, S. Coppola, and L. Ghibelli, "Possible involvement of poly(ADP-ribosyl) polymerase in triggering stress-induced apoptosis," *Experimental Cell Research*, vol. 212, no. 2, pp. 367–373, 1994.
- [23] C. S. Huang, W. R. Moore, and A. Meister, "On the active site thiol of gamma-glutamylcysteine synthetase: relationships to catalysis, inhibition, and regulation," *Proceedings of the National Academy of Sciences of the United States of America*, vol. 85, no. 8, pp. 2464–2468, 1988.
- [24] P. J. Dierickx, G. van Nuffel, and I. Alvarez, "Glutathione protection against hydrogen peroxide, tert-butyl hydroperoxide and diamide cytotoxicity in rat hepatoma-derived Fa32 cells," *Human & Experimental Toxicology*, vol. 18, no. 10, pp. 627–633, 1999.
- [25] T. Wood, "Preparation, properties, and analysis of the intermediates of the pathway," in *The Pentose Phosphate Pathway*, T. Wood, Ed., pp. 17–45, Academic Press, Orlando, FL, USA, 1985.
- [26] J. F. Williams, P. F. Blackmore, and K. K. Arora, "The significance of sedoheptulose 1, 7-bisphosphate in the metabolism and regulation of the pentose pathway in liver," *Biochemistry International*, vol. 11, no. 4, pp. 599–610, 1985.
- [27] M. F. Clasquin, E. Melamud, A. Singer et al., "Riboneogenesis in yeast," *Cell*, vol. 145, no. 6, pp. 969–980, 2011.
- [28] J. P. Richard, "Mechanism for the formation of methylglyoxal from triosephosphates," *Biochemical Society Transactions*, vol. 21, no. 2, pp. 549–553, 1993.
- [29] P. J. Thornalley, "Glyoxalase I—structure, function and a critical role in the enzymatic defence against glycation," *Biochemical Society Transactions*, vol. 31, no. 6, pp. 1343–1348, 2003.
- [30] P. J. Thornalley, "Protein and nucleotide damage by glyoxal and methylglyoxal in physiological systems—role in ageing and disease," *Drug Metabolism and Drug Interactions*, vol. 23, no. 1-2, pp. 125–150, 2008.
- [31] A. R. Hipkiss, "NAD⁺ availability and proteotoxicity," *Neuro-molecular Medicine*, vol. 11, no. 2, pp. 97–100, 2009.
- [32] S. Tshori, E. Razin, and H. Nechushtan, "Amino-acyl tRNA synthetases generate dinucleotide polyphosphates as second messengers: functional implications," *Topics in Current Chemistry*, vol. 344, pp. 189–206, 2014.
- [33] H. C. Pace, P. N. Garrison, A. K. Robinson et al., "Genetic, biochemical, and crystallographic characterization of Fhit-substrate complexes as the active signaling form of Fhit," *Proceedings of the National Academy of Sciences of the United States of America*, vol. 95, no. 10, pp. 5484–5489, 1998.
- [34] J. Pintor, M. Diaz-Hernandez, J. Gualix, R. Gomez-Villafuertes, F. Hernando, and M. T. Miras-Portugal, "Diadenosine polyphosphate receptors: from rat and guinea-pig brain to human nervous system," *Pharmacology & Therapeutics*, vol. 87, no. 2-3, pp. 103–115, 2000.
- [35] B. K. Pliyev, T. V. Dimitrieva, and V. G. Savchenko, "Diadenosine diphosphate (Ap₂A) delays neutrophil apoptosis via the adenosine A_{2A} receptor and cAMP/PKA pathway," *Biochemistry and Cell Biology*, vol. 92, no. 5, pp. 420–424, 2014.
- [36] J. Jankowski, J. Hagemann, M. Tepel et al., "Dinucleotides as growth-promoting extracellular mediators: presence of dinucleoside diphosphates Ap₂A, Ap₂G, and Gp₂G in releasable granules of platelets," *Journal of Biological Chemistry*, vol. 276, no. 12, pp. 8904–8909, 2001.
- [37] H. X. Yuan, Y. Xiong, and K. L. Guan, "Nutrient sensing, metabolism, and cell growth control," *Molecular Cell*, vol. 49, no. 3, pp. 379–387, 2013.
- [38] D. G. Hardie and S. C. Lin, "AMP-activated protein kinase – not just an energy sensor," *F1000Research*, vol. 6, p. 1724, 2017.
- [39] D. G. Hardie, "Sensing of energy and nutrients by AMP-activated protein kinase," *American Journal of Clinical Nutrition*, vol. 93, no. 4, pp. 891S–896S, 2011.
- [40] M. Lopez, "AMPK wars: the VMH strikes back, return of the PVH," *Trends in Endocrinology and Metabolism*, vol. 29, no. 3, pp. 135–137, 2018.
- [41] R. Rafaeloff-Phail, L. Ding, L. Conner et al., "Biochemical regulation of mammalian AMP-activated protein kinase activity by NAD and NADH," *Journal of Biological Chemistry*, vol. 279, no. 51, pp. 52934–52939, 2004.

- [42] B. Xiao, M. J. Sanders, E. Underwood et al., "Structure of mammalian AMPK and its regulation by ADP," *Nature*, vol. 472, no. 7342, pp. 230–233, 2011.
- [43] S. Cardaci, G. Filomeni, and M. R. Ciriolo, "Redox implications of AMPK-mediated signal transduction beyond energetic clues," *Journal of Cell Science*, vol. 125, no. 9, pp. 2115–2125, 2012.
- [44] B. Sid, J. Verrax, and P. B. Calderon, "Role of AMPK activation in oxidative cell damage: implications for alcohol-induced liver disease," *Biochemical Pharmacology*, vol. 86, no. 2, pp. 200–209, 2013.
- [45] O. H. Kang, M. Y. Shon, R. Kong et al., "Anti-diabetic effect of black ginseng extract by augmentation of AMPK protein activity and upregulation of GLUT2 and GLUT4 expression in db/db mice," *BMC Complementary and Alternative Medicine*, vol. 17, no. 1, p. 341, 2017.
- [46] A. S. Marsin, L. Bertrand, M. H. Rider et al., "Phosphorylation and activation of heart PFK-2 by AMPK has a role in the stimulation of glycolysis during ischaemia," *Current Biology*, vol. 10, no. 20, pp. 1247–1255, 2000.
- [47] M. L. Circu, R. E. Maloney, and T. Y. Aw, "Disruption of pyridine nucleotide redox status during oxidative challenge at normal and low-glucose states: implications for cellular adenosine triphosphate, mitochondrial respiratory activity, and reducing capacity in colon epithelial cells," *Antioxidants & Redox Signaling*, vol. 14, no. 11, pp. 2151–2162, 2011.
- [48] N. Pollak, M. Niere, and M. Ziegler, "NAD kinase levels control the NADPH concentration in human cells," *Journal of Biological Chemistry*, vol. 282, no. 46, pp. 33562–33571, 2007.
- [49] J. H. Grose, L. Joss, S. F. Velick, and J. R. Roth, "Evidence that feedback inhibition of NAD kinase controls responses to oxidative stress," *Proceedings of the National Academy of Sciences of the United States of America*, vol. 103, no. 20, pp. 7601–7606, 2006.
- [50] A. Chiarugi and M. A. Moskowitz, "PARP-1—a perpetrator of apoptotic cell death?," *Science*, vol. 297, no. 5579, pp. 200–201, 2002.
- [51] D. D'Amours, F. R. Sallmann, V. M. Dixit, and G. G. Poirier, "Gain-of-function of poly (ADP-ribose) polymerase-1 upon cleavage by apoptotic proteases: implications for apoptosis," *Journal of Cell Science*, vol. 114, Part 20, pp. 3771–3778, 2001.
- [52] D. Cantu, J. Schaack, and M. Patel, "Oxidative inactivation of mitochondrial aconitase results in iron and H₂O₂-mediated neurotoxicity in rat primary mesencephalic cultures," *PLoS One*, vol. 4, no. 9, p. e7095, 2009.
- [53] P. R. Gardner and I. Fridovich, "Superoxide sensitivity of the *Escherichia coli* aconitase," *Journal of Biological Chemistry*, vol. 266, no. 29, pp. 19328–19333, 1991.
- [54] J. Du, A. Yanagida, K. Knight et al., "Reductive carboxylation is a major metabolic pathway in the retinal pigment epithelium," *Proceedings of the National Academy of Sciences of the United States of America*, vol. 113, no. 51, pp. 14710–14715, 2016.